Synthesis of Sulfur-Resistant TiO$_2$-CeO$_2$ Composite and Its Catalytic Performance in the Oxidation of a Soluble Organic Fraction from Diesel Exhaust

Na Zhang [1]**, Zhengzheng Yang** [1],*iD**, Zhi Chen** [1]**, Yunxiang Li** [1]**, Yunwen Liao** [1,2]**, Youping Li** [1]**, Maochu Gong** [3] **and Yaoqiang Chen** [3],*

[1] College of Environmental Science and Engineering, China West Normal University, Nanchong 637009, China; nzhang@cwnu.edu.cn (N.Z.); ZCHEN0211@gmail.com (Z.C.); yx_li@cwnu.edu.cn (Y.L.); liao-yw@163.com (Y.L.); lyp920@163.com (Y.L.)

[2] Chemical Synthesis and Pollution Control Key Laboratory of Sichuan Province, College of Chemistry and Chemical Engineering, China West Normal University, Nanchong 637009, China

[3] Key Laboratory of Green Chemistry & Technology of the Ministry of Education, College of Chemistry, Sichuan University, Chengdu 610064, China; gongmaochu@scu.edu.cn

* Correspondence: zyang@cwnu.edu.cn (Z.Y.); nic7501@scu.edu.cn (Y.C.); Tel./Fax: +86-81-7256-8646 (Z.Y.); +86-28-8541-8451 (Y.C.)

check for updates

Abstract: Sulfur poisoning is one of the most important factors deteriorating the purification efficiency of diesel exhaust after-treatment system, thus improving the sulfur resistibility of catalysts is imperative. Herein, ceria oxygen storage material was introduced into a sulfur-resistant titania by a co-precipitation method, and the sulfur resistibility and catalytic activity of prepared TiO$_2$-CeO$_2$ composite in the oxidation of diesel soluble organic fraction (SOF) were studied. Catalytic performance testing results show that the CeO$_2$ modification significantly improves the catalytic SOF purification efficiency of TiO$_2$-CeO$_2$ catalyst. SO$_2$ uptake and energy-dispersive X-ray (EDX) results suggest that the ceria doping does not debase the excellent sulfur resistibility of bare TiO$_2$, the prepared TiO$_2$-CeO$_2$ catalyst exhibits obviously better sulfur resistibility than the CeO$_2$ and commercial CeO$_2$-ZrO$_2$-Al$_2$O$_3$. X-ray powder diffraction (XRD) and Raman spectra indicate that cerium ions can enter into the TiO$_2$ lattice and not form complete CeO$_2$ crystals. X-ray photoelectron spectroscopy (XPS), H$_2$-temperature programmed reduction (H$_2$-TPR) and oxygen storage capacity (OSC) testing results imply that the addition of CeO$_2$ in TiO$_2$-CeO$_2$ catalyst can significantly enhance the surface oxygen concentration and oxygen storage capacity of TiO$_2$-CeO$_2$.

Keywords: cerium-doped titania; sulfur-tolerant materials; organic compounds purification; diesel oxidation catalyst; vehicle exhaust

1. Introduction

Diesel engines have been widely used in passenger cars and vans, due to excellent fuel efficiency and durability. However, diesel exhaust gases, such as carbon monoxide (CO), unburned hydrocarbons (HC$_x$), nitrogen oxides (NO$_x$), particulate matter (PM) and soluble organic fraction (SOF), are considered major sources of air pollutants [1–3]. Among these hazardous pollutants, SOF are the heavy liquid hydrocarbons (C > 16 [4,5], aromatics and oxygenated compounds [6]) adsorbed on soot, which mainly come from unburned fuel and lube oils [7,8]. The content of SOF is known to vary with engine operating conditions and can reach about 5–60% of the whole mass of the particulate matter [6,9–11]. Due to the fact that diesel SOF contains types of polycyclic aromatic hydrocarbons

(PAHs) [12,13] which are recognized as strong carcinogens [14,15], purifying the SOF from diesel exhaust is an important and essential work.

Diesel oxidation catalyst (DOC) was employed to accelerate the oxidation and purification of diesel exhaust gases of CO, HC_x and SOF. In recent decades, CeO_2-ZrO_2, Al_2O_3 and their mixed oxide-based catalysts were widely used as commercial DOC and displayed excellent catalytic CO and HC_x oxidation activity. Focusing on the purification of SOF, CeO_2-based oxygen storage materials (OSM) have been greatly impressed by considerable researchers due to the superior catalytic activity on hydrocarbons and SOF oxidation [16–18]. Meanwhile, controlled synthesized of nanostructured CeO_2-based catalysts and their catalytic performance in diesel soot oxidation are lucubrated [19,20]. However, CeO_2-based catalysts are easily poisoned by SO_2 [21–24]. And SO_2 is a subsistent in the diesel exhaust, since sulfur is present in almost all commercial diesel fuels [25–27], sulfur in fuels would be oxidized to SO_2 and then emitted from diesel engines [28,29]. Furthermore, sulfur poisoning resulting from sulfur species accumulation is more destructive, since even using ultra-low sulfur diesel (ULSD), cumulative exposure of a catalyst over its lifetime in a heavy-duty diesel may amount to kilograms of sulfur [30]. A large amount of sulfur species accumulation inevitably results in the blocking of channels of monolithic catalyst, and hence the strike of diesel exhaust after-treatment system. Thus, it is important and realistic for a diesel oxidation catalyst to improve the sulfur resistibility.

TiO_2 is known as an effective sulfur-resistant material [31–33], and our previous works [34–36] also prove that TiO_2-based diesel oxidation catalysts display excellent sulfur resistibility. However, TiO_2 is not active enough for catalytic diesel SOF combustion. Reports about the sulfur resistance catalyst for diesel SOF oxidation are still scarce. Considering all of this, in this work, CeO_2 was introduced in TiO_2 by a co-precipitation method, and its effects on sulfur resistibility and catalytic activity for diesel SOF combustion were investigated.

2. Results and Discussion

2.1. Sulfur Resistibility

The sulfur resistibility values of catalysts were measured by sulfur uptake testing. As shown in Figure 1, under SO_2 exposure, the weight of all samples increased with time; final weight increments tended to be flat after 1–3 h SO_2 exposure, except for CeO_2. After 4 h, chosen as representative exposure time of simulative 160,000 km vehicle aged catalyst, the final weight increments of TiO_2, TiO_2-CeO_2 and CeO_2 catalysts are 1.63 wt. %, 2.01 wt. % and 4.72 wt. %, respectively. The normalized sulfur uptake results are calculated by supposing 1 g of sample as standard, and the results are listed in Table 1. The normalized sulfur uptake values of TiO_2, TiO_2-CeO_2 and CeO_2 catalysts are 166 $\mu g/m^2$, 170 $\mu g/m^2$, and 891 $\mu g/m^2$, respectively. From the results it can be seen that the sulfur species accumulation is severe on CeO_2 catalyst but is slight on both TiO_2 and TiO_2-CeO_2 catalysts, which implies that the TiO_2-based catalysts (TiO_2 and TiO_2-CeO_2) present obviously better sulfur resistibility than the CeO_2 catalyst. Since the non-sulfating material of TiO_2 displays low SO_2 adsorption and hence relieves sulfate generation and exhibits superior sulfur resistibility [32,37]. Furthermore, the introduction of moderate amounts of ceria in TiO_2 has essentially no effect on the naturally excellent sulfur resistibility of TiO_2.

Table 1. Sulfur accumulation and normalized sulfur uptake of the TiO_2, TiO_2-CeO_2 and CeO_2 samples.

Samples	Surface Area [a] (m^2/g)	Sulfur Content (wt. %)		Normalized Sulfur Uptake [c] ($\mu g/m^2$)
		Sulfur Uptake	EDX [b]	
TiO_2	98	1.63	1.02	166
TiO_2-CeO_2	118	2.01	1.04	170
CeO_2	53	4.72	4.26	891

[a] Surface area was calculated by BET method from the N_2 adsorption-desorption results; [b] EDX results were obtained by detecting the simulative 160,000 km vehicle aged samples; [c] The normalized sulfur uptake = sulfur uptake/(100 × surface area) [37,38].
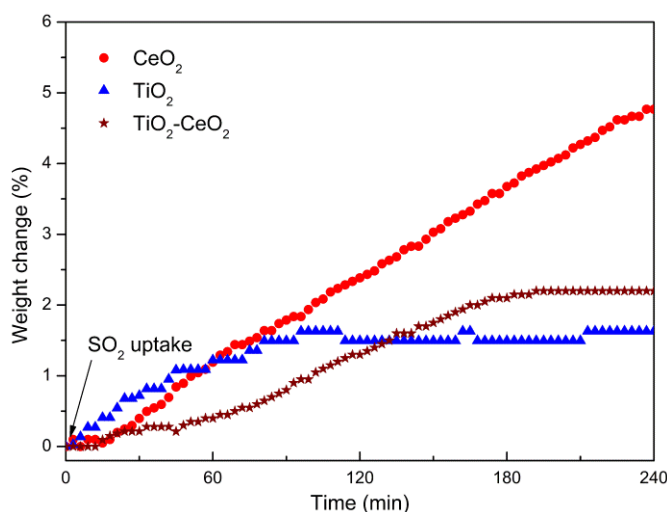
Figure 1. Sulfur uptake of the TiO_2, TiO_2-CeO_2 and CeO_2 catalysts.

Additionally, the accumulation amounts of sulfur species on simulative 160,000 km vehicle aged TiO_2, TiO_2-CeO_2 and CeO_2 catalysts tested by EDX (Table 1) are 1.02 wt. %, 1.04 wt. % and 4.26 wt. %, respectively, which shows the same trend with the sulfur uptake results. It is clear that the prepared TiO_2 and TiO_2-CeO_2 present significantly less sulfur species accumulation and better sulfur resistibility than the CeO_2 catalyst under the long-term exposure of diesel exhaust ambiences.

2.2. Catalytic Performance

Figure 2 shows the thermogravimetry-differential thermal analysis-differential thermogravimetry (TG-DTA-DTG) curves of the bulk lube without catalysts and the lube impregnated on catalysts; all of the DTA curves are the positive peaks indicating exothermic peaks, and all of the originally DTG negative peaks are inverted into positive peaks for a better readability of the graph. The combustion of lube without catalyst under air flow is shown in Figure 2a; the weight loss of bulk lube is tersely distinguished into two stages; about 90% of lube is deflagrated at 220–350 °C, and then the rest of 10% lubricating oil is consumed tardily after 350 °C till 500 °C, which implies that the commercial lube contains a fraction of hydrocarbons hard to pyrolyze (may come from the lubricant additive). The onset combustion temperature of $T_{10\%}$ (the temperature at which 10% of the initial lube is converted) is about 264 °C, the lube combustion fastest temperature of T_m (the temperature of weightlessness fastest point in DTG curves) is about 324 °C, and the final reaction temperature of T_f (the temperature of lube is completely converted) is about 507 °C. As shown in DTA curves of Figure 2a, a sharp and large exothermic peak is seen at about 325 °C which result from the rapid pyrolysis of bulk lube. Due to the decomposition of lube being an exothermic reaction, once ignition occurs, the heat continually increases and accumulates, and hence, most of lube is removed rapidly. The multiple peaks at 400–500 °C imply that the commercial lube contains multifarious hydrocarbons (lubricant additives) that are hard to decompose. Figure 2b plots the lubricant oxidation on CeO_2 catalyst. About 93% of the lube is rapidly oxidized between 140 °C and 280 °C, and the rest of 7% of lube is fully burnt at 280–340 °C. The onset combustion temperature of $T_{10\%}$ is about 162 °C, the fastest weightlessness temperature of T_m is about 186 °C and the final reaction temperature of T_f is about 322 °C. Figure 2c shows the decomposition of lubricant with TiO_2, the TG-DTG curves can be divided into four stages with different decomposition rates. About 16% of lube is decomposed at 205–266 °C, another 28% of the lube is burnt at 266–324 °C, about 49% of the lubricant is consumed at 324–396 °C and the rest of 7% of uninflammable lube is ignited between 396 °C and 420 °C. The onset combustion temperature of $T_{10\%}$ is about 249 °C, the final reaction temperature of T_f is about 420 °C, and three obviously fast weightlessness peaks of lube combustion are observed at about 252, 289 and 363 °C. For the TiO_2-CeO_2 catalyzed lube

combustion (Figure 2d), about 97% of the lubricating oil is rapidly combusted between 180 °C and 330 °C, and the rest of about 3% of lube is burnt out at 334–362 °C. The $T_{10\%}$, T_m and T_f is about 212, 261 and 362 °C, respectively.
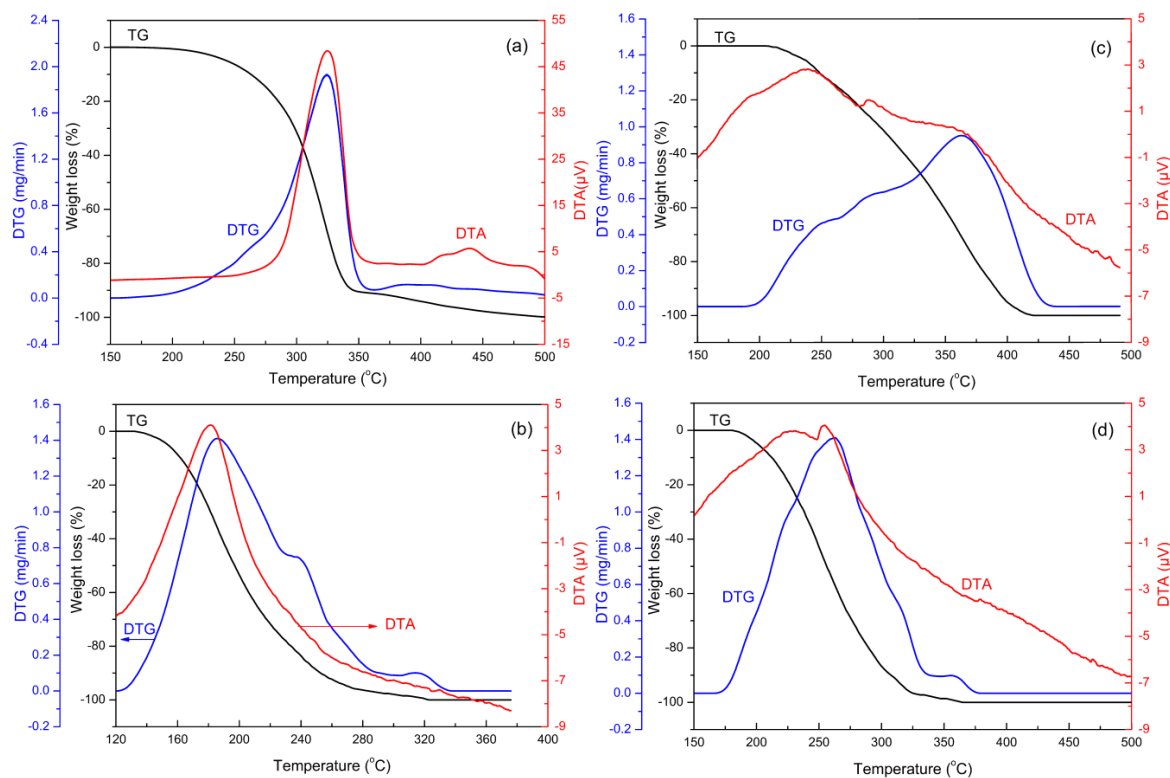

Figure 2. Simultaneous TG-DTA-DTG curves for simulating the catalytic performance for the combustion of SOF on (**a**) without catalyst; (**b**) CeO_2; (**c**) TiO_2 and (**d**) TiO_2-CeO_2 catalysts.

Due to the fact that the weight loss of lube can be ascribed either to evaporation or to combustion, the activity of prepared catalyst is also identified by the integrated area of the exotherm. The normalized DTA peak areas are described in units of μV·°C/(mg lube)/(mg sample), and then different catalysts can be directly compared on a common basis [39,40]. The larger the value of normalized DTA exotherm peak area, the greater the fraction of lubricant combusted verses evaporated, and the better the catalytic performance [39–41]. The oxidation activity data of catalysts for lube combustion are listed in Table 2. CeO_2 catalyst exhibits an outstanding catalytic lube oxidation activity, which is consistent with our previous reports [40,41]. Although the introduction of TiO_2 slightly lowers the combustion temperature of lube, bare TiO_2 is not active enough for catalytic SOF oxidation. About 60% of lube is burnt at 350 °C in the lube/TiO_2 sample, while the value of lube without catalyst sample is about 90%. This is because the lube oxidation is an exothermic reaction; once ignition occurs, the heat continually increases and accumulates. Thus, the burn of lube without catalyst (containing more lube oil) is more violently than the lube/TiO_2. The TiO_2-CeO_2 catalyst obviously lowers the onset temperature of lube combustion and considerably promote the removing of lube resulting from combustion. Compared to TiO_2, the prepared TiO_2-CeO_2 catalyst presents obviously lower SOF removal temperature and larger exothermal peak area, which indicates that the TiO_2-CeO_2 catalyst presents better catalytic lube combustion activity.

Table 2. Catalytic performances for the combustion of SOF over the prepared catalysts.

Samples	$T_{10\%}$ (°C)	T_m (°C)	T_f (°C)	Exothermal Peak Area (μV·°C/mg Lube)	Exothermal Peak Area (μV·°C/(mg Lube)/(mg Sample))
lube	264	324	507	283.9	-
lube/CeO$_2$	162	186	322	1068.1	119.5
lube/TiO$_2$	249	- [a]	420	901.6	102.6
lube/TiO$_2$-CeO$_2$	212	261	362	1029.5	115.5

[a] Three obviously fast weightlessness peaks are observed over the lube/TiO$_2$ sample.

2.3. Catalyst Characterization

2.3.1. XRD and Raman Spectra

The XRD patterns of prepared catalysts are shown in Figure 3; both TiO$_2$ and TiO$_2$-CeO$_2$ display only characteristic peaks which refer to the typical anatase structure of TiO$_2$. The peaks of TiO$_2$ are sharper than those of TiO$_2$-CeO$_2$, which indicates that the addition of CeO$_2$ impedes the crystal growth and sintering and lower crystallinity of the TiO$_2$-CeO$_2$ composite materials. In the case of TiO$_2$-CeO$_2$, the typical reflections of CeO$_2$ crystals at 28.7°, 33.2°, 47.7°, 56.6° and 77.1° are not observed, and the positions of typical anatase structure of TiO$_2$ shift obviously to smaller angles, which suggest that a complete CeO$_2$ crystal is not formed and Ce ions (Ce^{4+} radius: 0.087 nm) possibly enter into the TiO$_2$ (Ti^{4+} radius: 0.06 nm) lattice and resulting in an expansion of TiO$_2$ unit cell, the unit cell volume of anatase tetragonal cell of TiO$_2$ is 134.95 Å^3, for TiO$_2$-CeO$_2$, the value enlarges to 135.15 Å^3. Thus, it can be inferred that Ce ions entered into the TiO$_2$ unit cell, and this is a possible reason why the addition of ceria into TiO$_2$ has no effect on the naturally excellent sulfur resistibility of TiO$_2$.
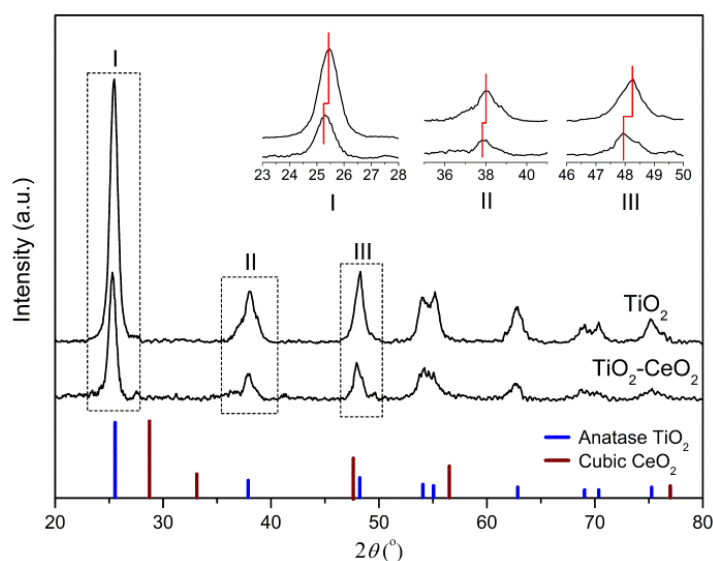

Figure 3. XRD patterns of the TiO$_2$ and TiO$_2$-CeO$_2$ catalysts.

To further confirm the above conjecture, Raman spectra were employed. As can be seen in Figure 4, CeO$_2$ presents a strong peak at about 464 cm^{-1}, which can be associated with the cubic CeO$_2$ [42]. TiO$_2$ and TiO$_2$-CeO$_2$ catalysts show five visible peaks at 145, 196, 397, 517 and 639 cm^{-1}, which are the A1g + 2B1g + 3Eg Raman-active modes of TiO$_2$ anatase phase (the peak at 517 cm^{-1} is complex of A$_{1g}$ and B$_{1g}$) [43], for the TiO$_2$-CeO$_2$ catalyst, the characteristic Raman peak of CeO$_2$ at 464 cm^{-1} is not observed. This result further confirmed that a CeO$_2$ crystal is not formed in the TiO$_2$-CeO$_2$ catalyst, which is consistent with the XRD result.
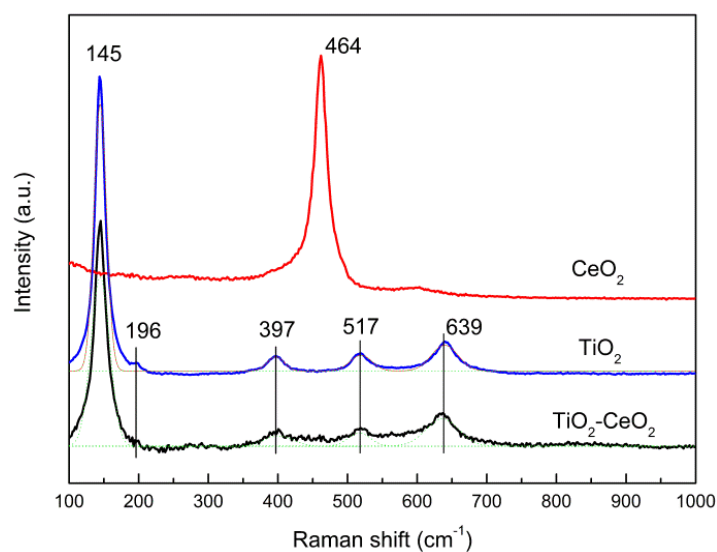
Figure 4. Raman spectra of the CeO_2, TiO_2 and TiO_2-CeO_2 catalysts.

2.3.2. Nitrogen Adsorption-Desorption

The nitrogen adsorption–desorption isotherms and pore size dispersion of TiO_2 and TiO_2-CeO_2 are shown in Figure 5; both TiO_2 and TiO_2-CeO_2 are mesoporous materials and show distinct H3 and H4 complex hysteresis loops indicating slit pore features; compared to TiO_2, the prepared TiO_2-CeO_2 displays obviously larger pore size; the textual features are listed in Table 3.
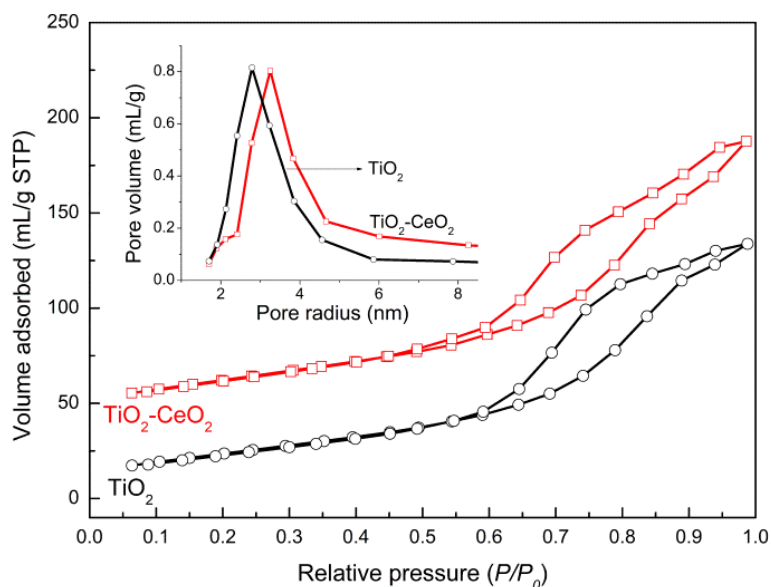

Figure 5. Nitrogen adsorption-desorption isotherms and pore size dispersion (inset) of the TiO_2 and TiO_2-CeO_2 catalysts.

Table 3. The texture properties of TiO_2 and TiO_2-CeO_2 catalysts.

Samples	Surface Area (m^2/g)	Pore Volume (cm^3/g)	Average Pore Diameter (nm)
TiO_2	98	0.22	7.2
TiO_2-CeO_2	118	0.26	8.6

The surface areas of TiO_2 and TiO_2-CeO_2 catalysts are about 98 m^2/g and 118 m^2/g, respectively, which indicates that the introduction of CeO_2 slightly increases the surface area of TiO_2. The pore volume and average pore size of TiO_2 are about 0.22 cm^3/g and 7.2 nm, respectively; the pore volume and average pore diameter of TiO_2-CeO_2 catalyst are 0.26 cm^3/g and 8.6 nm, respectively. It can be seen that the addition of CeO_2 to TiO_2 increases its surface area, pore volume and average pore size; this is possibly due to the addition of CeO_2 which impedes crystal growth and sintering and lowers crystallinity of the TiO_2-CeO_2 composite materials, and this speculation is consistent with the XRD results (Figure 3). The larger surface area, pore volume and pore size can be advantages to the contacting, transmitting and diffusion of the lube molecules on the catalyst, and hence, be beneficial to the catalytic SOF oxidation activity.

2.3.3. XPS

Figure 6 shows the XPS spectra of O 1s region of the CeO_2, TiO_2 and TiO_2-CeO_2 catalysts, all samples show two XPS peaks, the peak at about 530.1 eV can be assigned to lattice oxygen, and the peak with a binding energy of 532.1 eV is characteristic of surface adsorbed oxygen [37,44]. Due to the superior oxygen storage capacity, the peak of surface adsorbed oxygen of CeO_2 is obviously stronger than the lattice oxygen; the surface adsorbed oxygen ratio is about 55%. For the TiO_2 catalyst, the surface adsorbed oxygen ratio is about 38%, and the addition of CeO_2 obviously increases the surface adsorbed oxygen ratio, where the value of TiO_2-CeO_2 is about 42%. Usually, surface adsorbed oxygen is more reactive than lattice oxygen due to its higher mobility [45,46], and our previous work also confirms that the adsorbed oxygen is more active than the lattice oxygen in the catalytic SOF oxidation reaction [40]. Thus, the addition of CeO_2 in TiO_2 enhances the amounts of surface adsorbed oxygen of TiO_2-CeO_2, which can be responsible for the improved catalytic activity of SOF oxidation.

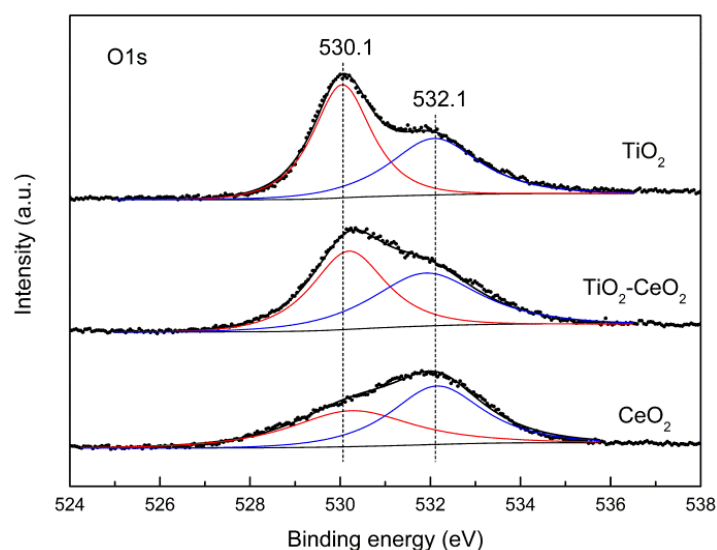**Figure 6.** XPS (O 1s) spectra of the CeO_2, TiO_2 and TiO_2-CeO_2 catalysts.

Additionally, the XPS (Ti2p) spectra of TiO_2 and TiO_2-CeO_2 catalysts are both located at 458.5 eV ($2p_{3/2}$) and 464.2 eV ($2p_{1/2}$), which are characteristic of TiO_2 species. Compared to bare CeO_2, the cerium peaks of TiO_2-CeO_2 are very weak and indiscernible, which indicates that the surface concentration of Ce in TiO_2-CeO_2 catalyst is very low; this phenomenon further confirms that Ce dopants are not gathering on the surface and are possibly entering into TiO_2 lattice, which is consistent with the XRD results (Figure 3).

2.3.4. H$_2$-TPR

The redox property of a catalyst is closely related to the catalytic performance. The redox behavior of the prepared catalysts is described by hydrogen temperature-programmed reduction (H$_2$-TPR) and shown in Figure 7.
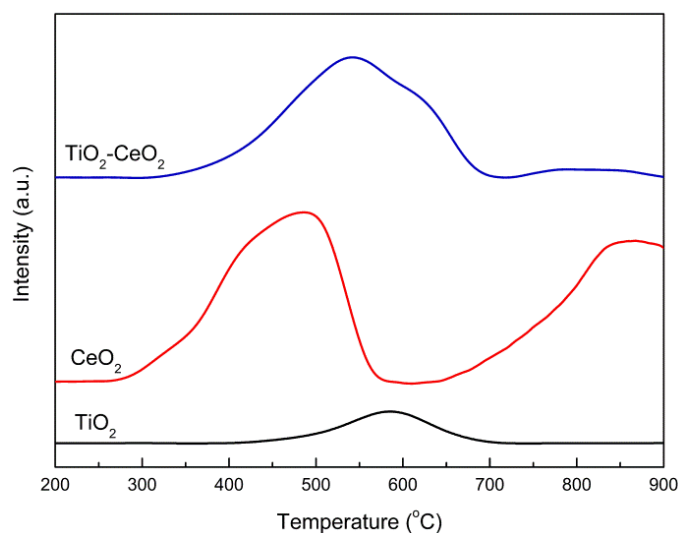

Figure 7. H$_2$-TPR profiles of the CeO$_2$, TiO$_2$ and TiO$_2$-CeO$_2$ catalysts.

The TPR peak of individual TiO$_2$ shows a weak peak at about 500–700 °C which may be ascribed to the reduction of TiO$_2$, and this phenomenon has been observed by other researchers [47,48]. The CeO$_2$ obviously shows a two-step reduction, the multiple low-temperature reduction peak at about 300–600 °C can be assigned to the reduction of surface oxygen, and the peak after 700 °C is ascribed to the reduction of CeO$_2$ bulk oxygen [47]. For the TiO$_2$-CeO$_2$, the reduction peak at 300–700 °C can be ascribed to the reduction of TiO$_2$ and surface oxygen of CeO$_2$; interestingly, the reduction peak of bulk oxygen of CeO$_2$ after 700 °C is poorly identified, which indicates that the TiO$_2$-CeO$_2$ catalyst exhibits lots of surface oxygen, and this result is consistent with XPS result. Consequently, the prepared TiO$_2$-CeO$_2$ catalyst with lots of surface oxygen species presents superior catalytic activity, due to the surface oxygen is highly reactive [45,46].

2.3.5. OSC

The CeO$_2$-based catalyst presents excellent oxygen storage capacity (OSC) and exhibits superior catalytic SOF oxidation activity [16,41]. The OSC of prepared catalysts were tested by an oxygen pulse injection technique and the results are listed in Table 4.

Table 4. The oxygen storage capacity (OSC) of TiO$_2$, TiO$_2$-CeO$_2$ and CeO$_2$-based catalysts.

Samples	OSC (µmol O$_2$/g Sample)	Normalized OSC (µmol O$_2$/g CeO$_2$)
TiO$_2$	2.9	-
TiO$_2$-CeO$_2$ [a]	101	524
CeO$_2$	73	73
Ce$_{0.35}$Zr$_{0.60}$Nd$_{0.05}$O$_2$	269 [49]	638

[a] The prepared TiO$_2$-CeO$_2$ catalyst in this work is Ce$_{0.1}$Ti$_{0.9}$O$_2$.

It can be seen that the OSC of TiO$_2$ is about 2.9 µmol/g, which is very slight and may be within the measurement uncertainties. While the addition of CeO$_2$ significantly increases the OSC of TiO$_2$-CeO$_2$ catalyst, the OSC is about 101 (µmol O$_2$)/(g sample), and the normalized OSC of TiO$_2$-CeO$_2$ catalyst is

about 524 (μmol O_2)/(g CeO_2). For the pure CeO_2 sample, the OSC is about 73 (μmol O_2)/(g sample). It should be mentioned that the static oxygen storage capacity testing for OSC of pure CeO_2 is an undervalued result, due to the oxygen mobility of bare CeO_2 being very low. Thus, a CeO_2-based oxygen storage materials in our previous work [49] is used as reference, the normalized OSC of $Ce_{0.35}Zr_{0.60}Nd_{0.05}O_2$ is about 638 (μmol O_2)/(g CeO_2). It can be seen that the normalized OSC of prepared TiO_2-CeO_2 catalyst is almost as good as the CeO_2-based oxygen storage materials. Based on the results, it can be suggested that although Ce ions enter into the TiO_2 lattice, the OSC of CeO_2 in TiO_2 is not degraded, the TiO_2-CeO_2 still exhibits good OSC. The good OSC of TiO_2-CeO_2 is one of the reasons that TiO_2-CeO_2 catalyst presents excellent catalytic SOF oxidation activity, this is consistent with the catalytic performance results (Figure 2 and Table 2) and the reports [16,41].

3. Materials and Methods

3.1. Catalyst Preparation

The TiO_2-CeO_2 catalyst was prepared by a co-precipitation method. Desired $TiOSO_4 \cdot 2H_2O$ and $Ce(NO_3)_3 \cdot 9H_2O$ mixture solutions with the molar ratio of Ti:Ce = 9:1, which was the optimal ratio to expose the single TiO_2 crystal structure in our previous studies [35,36], were slowly added to $NH_3 \cdot H_2O$ solutions under vigorous stirring. And then the precipitate was filtered and washed many times, after dried at 120 °C overnight and calcined for 3 h at 500 °C under airflow, the TiO_2-CeO_2 catalyst powder was obtained. The TiO_2 and CeO_2 catalysts were prepared by the same method.

The simulative 160,000 km vehicle aged sample was obtained by following reference [50] and our previous works [35,37]. Fresh catalyst was placed in a reactor and aged at 670 °C for 15 h and then at 250 °C for 15 h in the gases mixture at flow rate of 800 mL/min: 600 ppm C_3H_6, 1500 ppm CO, 200 ppm NO, 50 ppm SO_2, 5% O_2, 4% CO_2, 8% vapor and N_2 balance.

3.2. Catalyst Evaluation

The catalytic activity for SOF combustion of prepared catalysts were tested using TG-DTA method [16,39]. Due to the fact that the diesel SOF is comprised primarily of lube with a small amount of unburned fuel [51], commercial lubricating oil was often used to simulate the diesel SOF catalytic combustion [16,39].

For this test, the prepared powder catalyst was dried overnight at 120 °C to remove the effects of surface adsorbed water, and then impregnated with 5.0 wt. % commercial lube (Shell Helix HX7 5W-40, Shell Petrochemicals Company Limited, Jiaxing, China), the slurry of lube/catalyst mixture was stirred and mixed till a homogeneous state was obtained. About 10 mg of the lube/catalyst mixture powder was placed in the sample pan of TG-DTA unit (HCT-2, Beijing Henven Instruments, Beijing, China) and dried at 120 °C for 1 h to eliminate the effects of adsorbed substances (water, volatile matters etc.), and then heated to 550 °C with a temperature rate of 5 °C/min under airflow at 30 mL/min. The TG-DTA curves were recorded to determine the catalytic performance for SOF combustion of the prepared catalysts.

The test on lube without catalyst was carried out as a reference. About 10 mg of the lube was placed in the sample pan of TG-DTA unit and dried at 120 °C for 1 h, and then heated to 550 °C with a temperature rate of 5 °C/min under airflow at 30 mL/min.

3.3. Catalyst Characterization

Sulfur uptake was tested on a thermogravimetric analyzer (TGA) HCT-2 (Henven Instruments, Beijing, China). Consulting the references [38,52] and our previous works [37,53], about 15 mg of catalyst was placed in the sample crucible and pretreated under a 35 mL/min of N_2 flow for 5 h at 300 °C, and then the gas mixture of 43 mL/min SO_2(0.05 vol. %)-N_2 and 31 mL/min O_2(15.0 vol. %)-N_2 was introduced at 300 °C for 4 h, the weight increase as a function of time was recorded by the TGA.

The sulfur cumulant of catalysts after mimicking 160,000 km vehicle aging were analyzed by an energy-dispersive X-ray (EDX) spectroscopy (IE-250, Oxford Instruments, Oxford, UK).

X-ray powder diffraction (XRD) patterns were collected on a powder X-ray diffractometer (DX-1000, Dandong Fangyuan Instrument Ltd., Dandong, China) employing Cu Kα radiation (λ = 0.1542 nm).

Raman spectra were recorded by a LabRAM HR Laser Raman spectrometer (HORIBA Jobin Yvon Inc., Paris, France) with an excitation wavelength of 532 nm.

N_2 adsorption-description isotherms were measured on a QUADRASORB SI automated surface area and pore size analyzer (Quantachrome Instruments Ltd., Boynton Beach, FL, USA). The specific surface area and pore size were calculated by the Brunauer-Emmett-Teller (BET) method and Barret-Joyner-Halenda (BJH) method, respectively. Before adsorption measurements, the samples were degassed at 300 °C for 3 h under vacuum.

X-ray photoelectron spectroscopy (XPS) data were collected on a Kratos XSAM 800 spectrometer (Kratos Analytic Inc., Manchester, UK) with Al Kα radiation. The binding energy shifts of the samples were calibrated by fixing the C1s binding energy (BE 284.8 eV).

H_2-temperature programmed reduction (H_2-TPR) experiments were performed in a quartz tubular reactor. Samples were pretreated at 450 °C for 1 h under the N_2 flow (35 mL/min) and then cooled to room temperature; after that, the samples were heated from room temperature to 800 °C with a heating rate of 10 °C/min under the flow of H_2 (5.0 vol. %)-N_2 mixture. The hydrogen consumption as a function of reduction temperature was recorded by a thermal conductivity detector (TCD) cell.

The oxygen storage capacity (OSC) of the samples was measured by a pulse injection technique [54]. The sample was firstly reduced in a H_2 flow (30 mL/min) at 550 °C for 1 h; after cooling to 200 °C, an oxygen pulse was injected every 5 min to obtain a breakthrough curve, from which the OSC was calculated.

4. Conclusions

From the aforementioned results, it can be concluded that moderate amounts of ceria dopants in titania can obviously enhance the catalytic SOF oxidation activity of TiO_2-CeO_2 catalyst. Meanwhile, the prepared TiO_2-CeO_2 catalyst can maintain the naturally excellent sulfur resistibility of titania; the sulfur resistibility of TiO_2-CeO_2 is as well as the bare TiO_2. The prepared TiO_2-CeO_2 catalyst significantly enhances the sulfur tolerance of conventional CeO_2-based SOF oxidation catalysts and displays a good catalytic SOF oxidation activity. The TiO_2-CeO_2 catalyst exhibits a typical phase of anatase, and the cerium ions can enter into the TiO_2 unit cell, impede the crystal growth and sintering and lower crystallinity of the TiO_2-CeO_2 composite materials and, hence, improve the surface area, pore volume and pore size of TiO_2-CeO_2 catalyst. Moreover, the addition of CeO_2 in TiO_2 can significantly enhance the surface oxygen concentration and oxygen storage capacity of TiO_2-CeO_2; the normalized oxygen storage capacity of TiO_2-CeO_2 is almost as good as the CeO_2-based oxygen storage materials. The improvement of textual features and surface oxygen concentration of TiO_2-CeO_2 catalyst are the main reasons for the enhancement of catalytic SOF oxidation activity.

Author Contributions: Z.Y. and Y.C. conceived the project; N.Z., Z.Y. and Z.C. performed the experiments; Y.L. (Yunxiang Li), Y.L. (Yunwen Liao), Y.L. (Youping Li) and M.G. carried out the data analysis; N.Z. and Z.Y. wrote the paper.

Conflicts of Interest: The authors declare no conflict of interest.

References

1. Johnson, T.; Joshi, A. *Review of Vehicle Efficiency and Emissions*; SAE Technical Paper, 2017-01-0907; SAE: Warrendale, PA, USA, 2017.

2. Wang, X.; Westermann, A.; Shi, Y.; Cai, N.; Rieu, M.; Viricelle, J.-P.; Vernoux, P. Electrochemical Removal of NO_x on Ceria-Based Catalyst-Electrodes. *Catalysts* **2017**, *7*, 61. [CrossRef]

3. Godoy, M.; Banús, E.; Sanz, O.; Montes, M.; Miró, E.; Milt, V. Stacked Wire Mesh Monoliths for the Simultaneous Abatement of VOCs and Diesel Soot. *Catalysts* **2018**, *8*, 16. [CrossRef]

4. Williams, P.T.; Abbass, M.K.; Tarn, L.P.; Andrews, G.E.; Ng, K.L.; Bartle, K.D. *A Comparison of Exhaust Pipe, Dilution Tunnel and Roadside Diesel Particulate SOF and Gaseous Hydrocarbon Emissions*; SAE Technical Paper, 880351; SAE: Warrendale, PA, USA, 1988.

5. Osada, H.; Aoyagi, Y.; Shimada, K.; Akiyama, K.; Goto, Y.; Suzuki, H. *SOF Component of Lubricant Oil on Diesel PM in a High Boosted and Cooled EGR Engine*; SAE Technical Paper, 2007-01-0123; SAE: Warrendale, PA, USA, 2007.

6. Collura, S.; Chaoui, N.; Azambre, B.; Finqueneisel, G.; Heintz, O.; Krzton, A.; Koch, A.; Weber, J. Influence of the soluble organic fraction on the thermal behaviour, texture and surface chemistry of diesel exhaust soot. *Carbon* **2005**, *43*, 605–613. [CrossRef]

7. Atribak, I.; Bueno-López, A.; García-García, A. Uncatalysed and catalysed soot combustion under $NO_x + O_2$: Real diesel versus model soots. *Combust. Flame* **2010**, *157*, 2086–2094. [CrossRef]

8. Farrauto, R.J.; Mooney, J.J. *Effects of Sulfur on Performance of Catalytic Aftertreatment Devices*; SAE Technical Paper, 920557; SAE: Warrendale, PA, USA, 1992.

9. Spezzano, P.; Picini, P.; Cataldi, D. Gas-and particle-phase distribution of polycyclic aromatic hydrocarbons in two-stroke, 50-cm^3 moped emissions. *Atmos. Environ.* **2009**, *43*, 539–545. [CrossRef]

10. Stanmore, B.R.; Brilhac, J.F.; Gilot, P. The oxidation of soot: A review of experiments, mechanisms and models. *Carbon* **2001**, *39*, 2247–2268. [CrossRef]

11. Clague, A.D.H.; Donnet, J.B.; Wang, T.K.; Peng, J.C.M. A comparison of diesel engine soot with carbon black1. *Carbon* **1999**, *37*, 1553–1565. [CrossRef]

12. Westerholm, R.; Christensen, A.; de Serves, C.; Almén, J. *Determination of Polycyclic Aromatic Hydrocarbons (PAH) in Size Fractionated Diesel Particles from a Light Duty Vehicle*; SAE Technical Paper, 1999-01-3533; SAE: Warrendale, PA, USA, 1999.

13. Hansen, K.F.; Jensen, M.G. *Chemical and Biological Characteristics of Exhaust Emissions from a DI Diesel Engine Fuelled with Rapeseed Oil Methyl Ester (RME)*; SAE Technical Paper, 971689; SAE: Warrendale, PA, USA, 1997.

14. Callén, M.; Iturmendi, A.; López, J.; Mastral, A. Source apportionment of the carcinogenic potential of polycyclic aromatic hydrocarbons (PAH) associated to airborne PM_{10} by a PMF model. *Environ. Sci. Pollut. Res.* **2014**, *21*, 2064–2076. [CrossRef] [PubMed]

15. Benbrahim-Tallaa, L.; Baan, R.A.; Grosse, Y.; Lauby-Secretan, B.; el Ghissassi, F.; Bouvard, V.; Guha, N.; Loomis, D.; Straif, K. Carcinogenicity of diesel-engine and gasoline-engine exhausts and some nitroarenes. *Lancet Oncol.* **2012**, *13*, 663–664. [CrossRef]

16. Farrauto, R.J.; Voss, K.E. Monolithic diesel oxidation catalysts. *Appl. Catal. B Environ.* **1996**, *10*, 29–51. [CrossRef]

17. Cao, Y.; Lan, L.; Feng, X.; Yang, Z.; Zou, S.; Xu, H.; Li, Z.; Gong, M.; Chen, Y. Cerium promotion on the hydrocarbon resistance of a Cu-SAPO-34 NH_3-SCR monolith catalyst. *Catal. Sci. Technol.* **2015**, *5*, 4511–4521. [CrossRef]

18. Huang, Y.-F.; Zhang, H.-L.; Yang, Z.-Z.; Zhao, M.; Huang, M.-L.; Liang, Y.-L.; Wang, J.-L.; Chen, Y.-Q. Effects of CeO_2 Addition on Improved NO Oxidation Activities of Pt/SiO_2-Al_2O_3 Diesel Oxidation Catalysts. *Acta Phys.-Chim. Sin.* **2017**, *33*, 1242–1252.

19. Sudarsanam, P.; Hillary, B.; Amin, M.H.; Rockstroh, N.; Bentrup, U.; Bruckner, A.; Bhargava, S.K. Heterostructured Copper-Ceria and Iron-Ceria Nanorods: Role of Morphology, Redox, and Acid Properties in Catalytic Diesel Soot Combustion. *Langmuir* **2018**, *34*, 2663–2673. [CrossRef] [PubMed]

20. Putla, S.; Amin, M.H.; Reddy, B.M.; Nafady, A.; Al Farhan, K.A.; Bhargava, S.K. MnO_x Nanoparticle-Dispersed CeO_2 Nanocubes: A Remarkable Heteronanostructured System with Unusual Structural Characteristics and Superior Catalytic Performance. *ACS Appl. Mater. Interfaces* **2015**, *7*, 16525–16535. [CrossRef] [PubMed]

21. Yang, Z.-Z.; Yang, Y.; Zhao, M.; Gong, M.-C.; Chen, Y.-Q. Enhanced Sulfur Resistance of Pt-Pd/CeO$_2$-ZrO$_2$-Al$_2$O$_3$ Commercial Diesel Oxidation Catalyst by SiO$_2$ Surface Cladding. *Acta Phys.-Chim. Sin.* **2014**, *30*, 1187–1193.

22. Kolli, T.; Kanerva, T.; Lappalainen, P.; Huuhtanen, M.; Vippola, M.; Kinnunen, T.; Kallinen, K.; Lepisto, T.; Lahtinen, J.; Keiski, R.L. The Effect of SO$_2$ and H$_2$O on the Activity of Pd/CeO$_2$ and Pd/Zr-CeO$_2$ Diesel Oxidation Catalysts. *Top. Catal.* **2009**, *52*, 2025–2028. [CrossRef]

23. Luo, T.; Gorte, R.J. Characterization of SO$_2$-poisoned ceria-zirconia mixed oxides. *Appl. Catal. B Environ.* **2004**, *53*, 77–85. [CrossRef]

24. Deshmukh, S.S.; Zhang, M.; Kovalchuk, V.I.; d'Itri, J.L. Effect of SO$_2$ on CO and C$_3$H$_6$ oxidation over CeO$_2$ and Ce$_{0.75}$Zr$_{0.25}$O$_2$. *Appl. Catal. B Environ.* **2003**, *45*, 135–145. [CrossRef]

25. Xia, Z.; Fu, J.; Duan, A.; Han, L.; Wu, H.; Zhao, Z.; Xu, C.; Wang, D.; Wang, B.; Meng, Q. Post Synthesis of Aluminum Modified Mesoporous TUD-1 Materials and Their Application for FCC Diesel Hydrodesulfurization Catalysts. *Catalysts* **2017**, *7*, 141. [CrossRef]

26. Zhang, M.H.; Fan, J.Y.; Chi, K.; Duan, A.J.; Zhao, Z.; Meng, X.L.; Zhang, H.L. Synthesis, characterization, and catalytic performance of NiMo catalysts supported on different crystal alumina materials in the hydrodesulfurization of diesel. *Fuel Process. Technol.* **2017**, *156*, 446–453. [CrossRef]

27. Zhang, K.; Hu, J.; Gao, S.; Liu, Y.; Huang, X.; Bao, X. Sulfur content of gasoline and diesel fuels in northern China. *Energy Policy* **2010**, *38*, 2934–2940. [CrossRef]

28. Corro, G. Sulfur impact on diesel emission control—A review. *React. Kinet. Catal Lett.* **2002**, *75*, 89–106. [CrossRef]

29. Zelenka, P.; Ostgathe, K.; Lox, E. *Reduction of Diesel Exhaust Emissions by Using Oxidation Catalysts*; SAE Technical Paper, 902111; SAE: Warrendale, PA, USA, 1990.

30. Li, J.; Kumar, A.; Chen, X.; Currier, N.; Yezerets, A. *Impact of Different Forms of Sulfur Poisoning on Diesel Oxidation Catalyst Performance*; SAE Technical Paper, 2013-01-0514; SAE: Warrendale, PA, USA, 2013.

31. Paulson, T.; Moss, B.; Todd, B.; Eckstein, C.; Wise, B.; Singleton, D.; Zemskova, S.; Silver, R. *New Developments in Diesel Oxidation Catalysts*; SAE Technical Paper, 2008-01-2638; SAE: Warrendale, PA, USA, 2008.

32. Kanno, Y.; Hihara, T.; Watanabe, T.; Katoh, K. *Low Sulfate Generation Diesel Oxidation Catalyst*; SAE Technical Paper, 2004-01-1427; SAE: Warrendale, PA, USA, 2004.

33. Ueno, H.; Furutani, T.; Nagami, T.; Aono, N.; Goshima, H.; Kasahara, K. *Development of Catalyst for Diesel Engine*; SAE Technical Paper, 980195; SAE: Warrendale, PA, USA, 1998.

34. Yang, Z.; Li, J.; Zhang, H.; Yang, Y.; Gong, M.; Chen, Y. Size-dependent CO and propylene oxidation activities of platinum nanoparticles on the monolithic Pt/TiO$_2$-YO$_x$ diesel oxidation catalyst under simulative diesel exhaust conditions. *Catal. Sci. Technol.* **2015**, *5*, 2358–2365. [CrossRef]

35. Yang, Z.; Zhang, N.; Cao, Y.; Gong, M.; Zhao, M.; Chen, Y. Effect of yttria in Pt/TiO$_2$ on sulfur resistance diesel oxidation catalysts: Enhancement of low-temperature activity and stability. *Catal. Sci. Technol.* **2014**, *4*, 3032–3043. [CrossRef]

36. Yang, Z.; Chen, Y.; Zhao, M.; Zhou, J.; Gong, M.; Chen, Y. Preparation and Properties of Pt/Zr$_x$Ti$_{1-x}$O$_2$ Catalysts with Low-Level SO$_2$ Oxidation Activity for Diesel Oxidation, Cuihua Xuebao. *Chin. J. Catal.* **2012**, *33*, 819–826. (In Chinese)

37. Yang, Z.; Zhang, N.; Cao, Y.; Li, Y.; Liao, Y.; Li, Y.; Gong, M.; Chen, Y. Promotional effect of lanthana on the high-temperature thermal stability of Pt/TiO$_2$ sulfur-resistant diesel oxidation catalysts. *RSC Adv.* **2017**, *7*, 19318–19329. [CrossRef]

38. Koranne, M.M.; Pryor, J.N. Sulfur Tolerant Alumina Catalyst Support. U.S. Patent 8,158,257, 17 April 2012.

39. Zhang, Z.; Zhang, Y.; Mu, Z.; Yu, P.; Ni, X.; Wang, S.; Zheng, L. Synthesis and catalytic properties of Ce$_{0.6}$Zr$_{0.4}$O$_2$ solid solutions in the oxidation of soluble organic fraction from diesel engines. *Appl. Catal. B Environ.* **2007**, *76*, 335–347. [CrossRef]

40. Yang, Y.; Yang, Z.Z.; Xu, H.D.; Xu, B.Q.; Zhang, Y.H.; Gong, M.C.; Chen, Y.Q. Influence of La on CeO$_2$-ZrO$_2$ Catalyst for Oxidation of Soluble Organic Fraction from Diesel Exhaust. *Acta Phys.-Chim. Sin.* **2015**, *31*, 2358–2365.

41. Chen, Y.-D.; Wang, L.; Guan, X.-X.; Liu, Y.-B.; Gong, M.-C.; Chen, Y.-Q. Catalytic Oxidation of Soluble Organic Fraction in Diesel Exhausts Using Composite Oxides (CeO$_2$)$_x$(La-Al$_2$O$_3$)$_{1-x}$. *Acta Phys.-Chim. Sin.* **2013**, *29*, 1048–1054.

42. Fornasiero, P.; Balducci, G.; di Monte, R.; Kašpar, J.; Sergo, V.; Gubitosa, G.; Ferrero, A.; Graziani, M. Modification of the Redox Behaviour of CeO_2 Induced by Structural Doping with ZrO_2. *J. Catal.* **1996**, *164*, 173–183. [CrossRef]

43. Balachandran, U.; Eror, N.G. Raman spectra of titanium dioxide. *J. Solid State Chem.* **1982**, *42*, 276–282. [CrossRef]

44. Sellick, D.R.; Aranda, A.; García, T.; López, J.M.; Solsona, B.; Mastral, A.M.; Morgan, D.J.; Carley, A.F.; Taylor, S.H. Influence of the preparation method on the activity of ceria zirconia mixed oxides for naphthalene total oxidation. *Appl. Catal. B Environ.* **2013**, *132–133*, 98–106. [CrossRef]

45. Xu, H.; Cao, Y.; Wang, Y.; Fang, Z.; Lin, T.; Gong, M.; Chen, Y. The influence of molar ratios of Ce/Zr on the selective catalytic reduction of NO_x with NH_3 over Fe_2O_3-WO_3/$Ce_xZr_{1-x}O_2$ ($0 \le x \le 1$) monolith catalyst. *Chin. Sci. Bull.* **2014**, *59*, 3956–3965. [CrossRef]

46. Wu, Z.; Jin, R.; Liu, Y.; Wang, H. Ceria modified MnO_x/TiO_2 as a superior catalyst for NO reduction with NH_3 at low-temperature. *Catal. Commun.* **2008**, *9*, 2217–2220. [CrossRef]

47. Zhu, H.; Qin, Z.; Shan, W.; Shen, W.; Wang, J. Pd/CeO_2–TiO_2 catalyst for CO oxidation at low temperature: A TPR study with H_2 and CO as reducing agents. *J. Catal.* **2004**, *225*, 267–277. [CrossRef]

48. Watanabe, S.; Ma, X.; Song, C. Characterization of Structural and Surface Properties of Nanocrystalline TiO_2−CeO_2 Mixed Oxides by XRD, XPS, TPR, and TPD. *J. Phys. Chem. C* **2009**, *113*, 14249–14257. [CrossRef]

49. Guo, J.; Shi, Z.; Wu, D.; Yin, H.; Gong, M.; Chen, Y. Effects of Nd on the properties of CeO_2–ZrO_2 and catalytic activities of three-way catalysts with low Pt and Rh. *J. Alloy. Compd.* **2015**, *621*, 104–115. [CrossRef]

50. Andersson, J.; Antonsson, M.; Eurenius, L.; Olsson, E.; Skoglundh, M. Deactivation of diesel oxidation catalysts: Vehicle- and synthetic aging correlations. *Appl. Catal. B Environ.* **2007**, *72*, 71–81. [CrossRef]

51. Voss, K.E.; Lampert, J.K.; Farrauto, R.J.; Rice, G.W.; Punke, A.; Krohn, R. Catalytic oxidation of diesel particulates with base metal oxides. *Stud. Surf. Sci. Catal.* **1995**, *96*, 499–515.

52. Koranne, M.M.; Pryor, J.N.; Chapman, D.M.; Brezny, R. Sulfur Tolerant Alumina Catalyst Support. U.S. Patent 8,076,263, 13 December 2011.

53. Yang, Z.; Li, Y.; Liao, Y.; Li, Y.; Zhang, N. Preparation and properties of the Pt/SiO_2-Al_2O_3 sulfur resistance diesel oxidation catalyst. *Environ. Chem.* **2016**, *35*, 1682–1689. (In Chinese)

54. Lan, L.; Chen, S.; Cao, Y.; Gong, M.; Chen, Y. New insights into the structure of a CeO_2-ZrO_2-Al_2O_3 composite and its influence on the performance of the supported Pd-only three-way catalyst. *Catal. Sci. Technol.* **2015**, *5*, 4488–4500. [CrossRef]